

Energy Stress of Metal Oxide Surge Arrester in GIS Substation Due to Shielding Failure

M. S. El-Bages, M. A. Abd-Allah, T. Elyan and Amira .G .Nawar

Electrical Engineering Department
Faculty of Engineering at Shoubra
Benha University

Abstract- High voltage metal oxide surge arresters (MOSA) are stressed by overvoltages generated in a power system. The selection of standard methods for the energy absorption capability of high voltage MOSA is based on the discharge energy estimation. This paper discusses the energy stresses of metal oxide surge arrester due to shielding failure. The energy stresses are calculated for arresters located inside 220/66/11 kV Wadi-Hoff gas insulated substation in the Egyptian network. A lightning stroke with different magnitudes is applied at different points along the line connected between Wadi-Hoff substation and Tebbin-power stations and the energy stress in each case is discussed. The effects of incoming and outgoing feeders types on FTO magnitudes and energy stresses are presented and discussed..

Index Terms- GIS, GIL, FTO, MOSA, Shielding Failure, ATP-EMTP simulation

I. INTRODUCTION

Due to the presence of overhead transmission lines within the power system, there is a risk that lightning strokes to, or immediately adjacent to the overhead lines, may result in dangerous overvoltage affecting on substation equipment. Lightning caused interruptions by shielding failures or by back-flashover. With effective shielding, it is possible to minimize direct strokes to the phase conductors, but this does not necessarily mean that the line will have satisfactory lightning performance. These shield failure currents plus currents from subsequent strokes produce arrester energies that normally exceed the energy caused by strokes to shield wire. A shielding failure event or a stroke to the conductor is essentially a single-phase event. The energy stress is much higher when the return stroke hits a phase conductor than when the impact is produced at a shield wire. Lightning currents are of smaller amplitudes, but they are directly striking the phase conductor and stressing the lightning surge arrester and in this case failure or damage can occur [1, 2].

Polymeric housed surge arresters are widely applied to power transmission systems in order to protect the systems from overvoltages. Various studies, have been done and show that polymer housed surge arresters are exposed to various stresses such as temporary overvoltages (TOV), switching overvoltages and lightning overvoltages. Due to these overvoltages and high currents, surge arrester will be stressed with energy which shouldn't exceed the arrester energy absorption capability which is the maximum level of energy injected into the arrester then it can cool back to its normal operating temperature. If the stresses exceeded, failure may occur, and damage the arrester due to thermal heating can produced inside arrester [3].

A single line diagram of 220/66/11 kV Wadi-Hoff double bus bar substation, used in this work, is shown in Fig. (1). It consists of four feeders, two feeders have a length of 30 km each, and the other two feeders have a length of 3 km each. The substation has 3x125MVA, 220/66/11 kV, power transformers. The feeders are connected to double bus bar with a bus coupler arrangement.

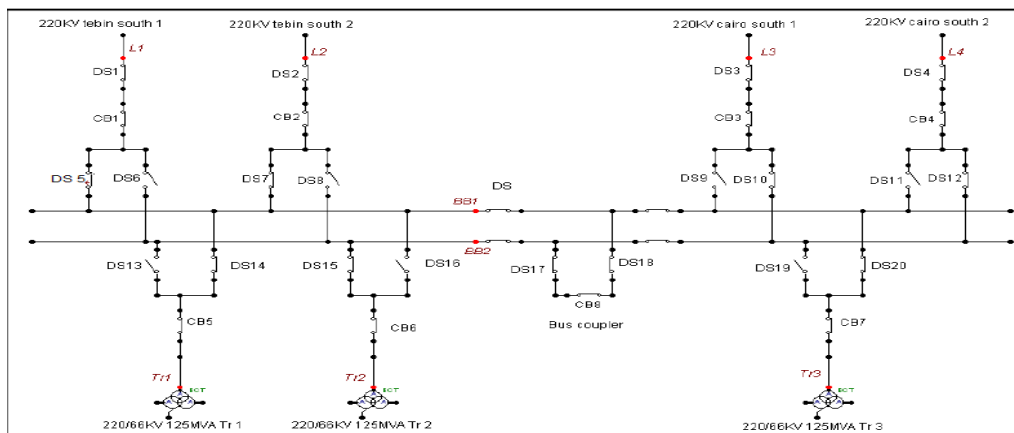


Figure 1: Typical single line diagram for Wadi-Hoff GIS

II. GIS SUBSTATION AND CONNECTED LINES MODELING

GIS installation can be regarded as series of distributed transmission lines and lumped capacitor elements. The values of each GIS section can be calculated from the standard formula of capacitance and inductance, treating the GIS as a concentric conductor [4, 5].

$$C = \frac{2\pi\epsilon}{\ln\left(\frac{R}{r}\right)} \quad (\epsilon \approx \epsilon_o) \quad \text{F/m} \quad (1)$$

$$L = \frac{\mu \ln\frac{R}{r}}{2\pi} \quad \text{H/m} \quad (2)$$

$$Z_1 = \sqrt{\frac{L}{C}} = \frac{\sqrt{\epsilon\mu}}{2\pi} \ln\frac{R}{r} \approx 60 \ln\frac{R}{r} \Omega \quad (3)$$

$$v = \frac{1}{\sqrt{LC}} \text{ m/s} \quad (4)$$

Where, C is capacitance of GIS bus bar per unit length, L is inductance of GIS bus bar per unit length, r is inside diameter of GIS enclosure, R is outside diameter of GIS bus bar, ϵ is absolute permittivity of SF_6 Gas (8.85×10^{-12}), μ is absolute permeability of copper conductor ($4\pi \times 10^{-7}$) and Z_1 is surge impedance.

The characteristic impedance and the propagation velocity of GIS busbar can be taken as 70Ω and $270\text{m}/\mu\text{s}$, respectively. The impedance of the circuit breaker in the closed position is taken as 70Ω , while in the opening position is taken as capacitances of 90pF from both end to ground and 50pF between contacts. The impedance of the disconnecter in the closed position is taken as 70Ω , while in the opening position is taken as capacitances of 30pF from both end to ground and 30 pF between contacts. The impedance of the potential transformer is taken as a capacitance of 100pF towards ground. The characteristic impedance and the propagation velocity of current transformer can be taken as 70Ω and $270\text{m}/\mu\text{s}$, respectively. The elbows, spacers, and spherical shields are simulated by a lumped capacitance of 15pF towards ground. The bushings are simulated by an impedance of 70Ω and a capacitance of 100 pF towards ground [5, 6, 7]. Lightning is simulated as an impulse current source of 10, 20, 30, 40 kA peak with an impulse waveform of $(1/50)\mu\text{s}$ in parallel with a resistance of 400Ω [8]. The 220 kV overhead transmission lines are modeled using ATP-EMTP and represented by distributed parameter model, using the JMARTI frequency dependent model Lines/Cables (LCC), which are the most accepted model for transient study [9]. The model of gapless type line surge arrester includes non-linear and dynamic behavior of the arrester and arrester is modeled as recommended Pinceti model. Lightning arrester is modeled by MOV-Type 92, as shown in Fig (2). The non-linear behavior was represented by the U-I characteristic depicted in Fig.(3) [10]. Surge arrester electrical data is shown in Table 1.

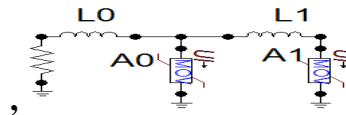


Figure 2: MOV-type 92 model

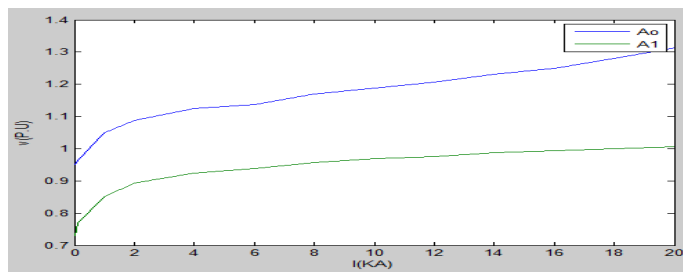


Figure 3: V-I characteristics of nonlinear A0 and A1

Table (1) Electrical data for line surge arrester

Rated voltage [kVrms]	Line discharge class	Lightning discharge capability [kJ]	Maximum residual voltage with current wave 8/20 μs [kV]			
			5 kA	10 kA	20 Ka	40 Ka
198	3	1568	453	476	524	586

III. OVERVOLTAGE ANALYSIS WITHOUT MOSA

The overvoltage transient is measured at the GIS terminal (L2) due to 1/50 μ s lightning stroke having 20kA peak current hit the feeder L2 at 1.0 km from GIS terminal is shown in Fig.(4). The overvoltage is oscillated and ceases to the normal system voltage after 17ms. The peak value of the transient overvoltage reaches at this terminal is 725kV. The peak values of the transient overvoltage reaches at the terminal L2 at different peak values of the 1/50 μ s striking impulse current is shown in Fig (5). It is seen that, as the lightning stroke current magnitude increases, the peak value of the fast transient overvoltage (FTO) will be increased.

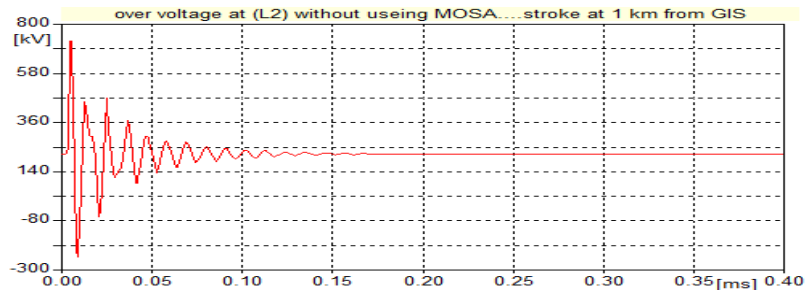


Figure 4: Fast transient overvoltage at GIS terminal (L2) due to 20 kA lightning stroke

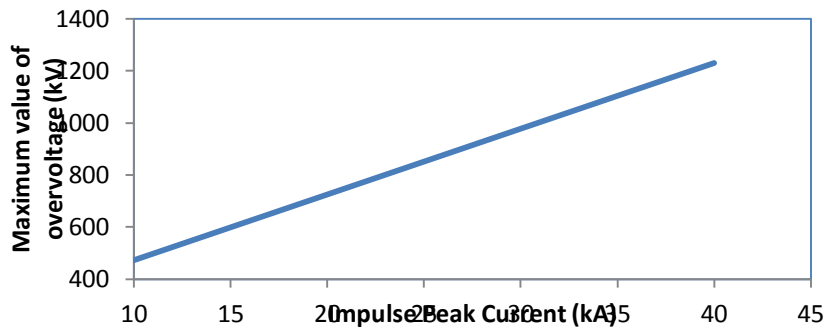
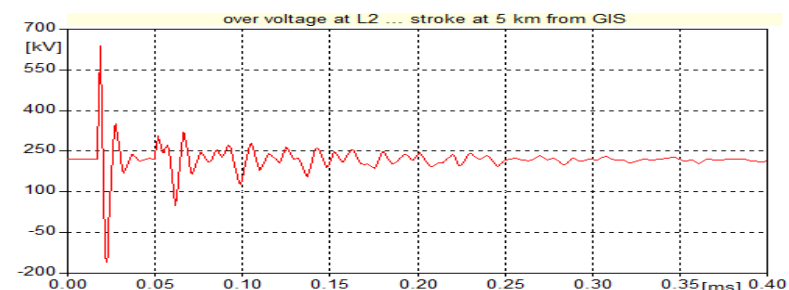
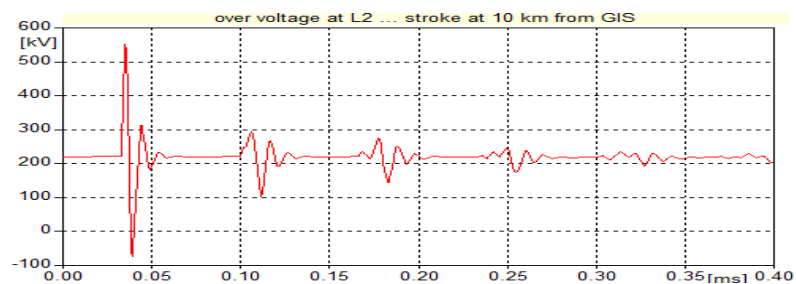


Figure 5: Overvoltage versus lightning stroke current without using MOSA

The lightning stroke of 20 kA peak and 1/50 μ s wave shape is assumed to hit the overhead transmission line at distances of 5 and 10 km from the GIS terminal. Fig.(6) shows the fast transient overvoltage at GIS terminal L2 for these different hitting points, while Fig.(5) shows the same lightning impulse hit the feeder at 1km. It can be seen that, as the distance between striking point and GIS terminal increases, the fast transient overvoltage is decreased, while the oscillations taken longer time.



(a) FTO at L2 when impulse hit the feeder at 5 km from GIS

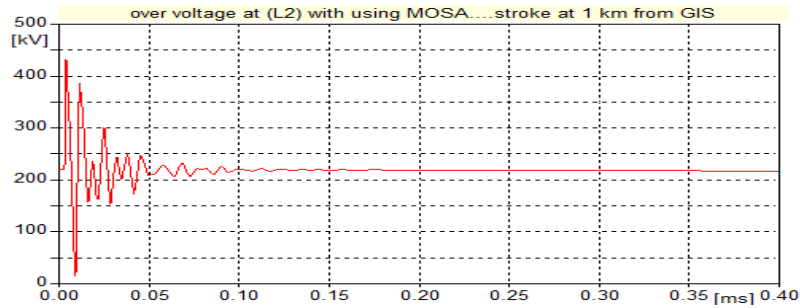


(b) FTO at L2 when impulse hit the feeder at 10 km from GIS

Figure 6: FTO due to 20 kA lightning stroke at different distances from GIS

IV. OVERVOLTAGE ANALYSIS WITH MOSA

The overvoltage transient when using MOSA at the GIS terminal (L2) due to $1/50\mu\text{s}$ lightning stroke, having 20kA peak current, hit the feeder L2 at 1.0 km from GIS terminal is shown in Fig.(7). It is seen that, MOSA is effectively reduces the magnitude of FTO at GIS terminal which will in turn reduces its effects on GIS components. The overvoltage is oscillated and ceases to the normal system voltage after 17ms. The peak value of the transient overvoltage reaches at this terminal is 431.9kV. The peak values of the transient overvoltage reaches at the terminal L2 at different peak values of the $1/50\mu\text{s}$ striking impulse current is shown in Fig(8). It is seen that, as the lightning stroke current magnitude increases, the peak value of the fast transient overvoltage (FTO) will be increased.



(a) FTO due to 20 kA lightning stroke with MOSA (431.9 kV)
 Figure 7: FTO at GIS terminal (L2) due to 20kA lightning strokes with using MOSA

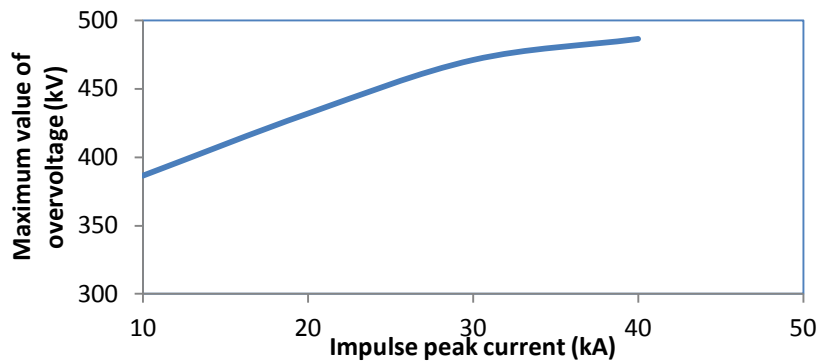


Figure 8: Overvoltage versus lightning stroke current with using MOSA

V. ENERGY STRESS OF MOSA

The energy stress of the MOSA is calculated when $1/50\mu\text{s}$ lightning wave strike the feeder L2 at a distance of 1.0 km from the GIS terminal at different peak lightning current stroke magnitudes. Fig.(9) shows the energy stress of MOSA versus the peak value of lightning current. As the peak value of the lightning current increases, the energy stress on MOSA is increased rapidly.

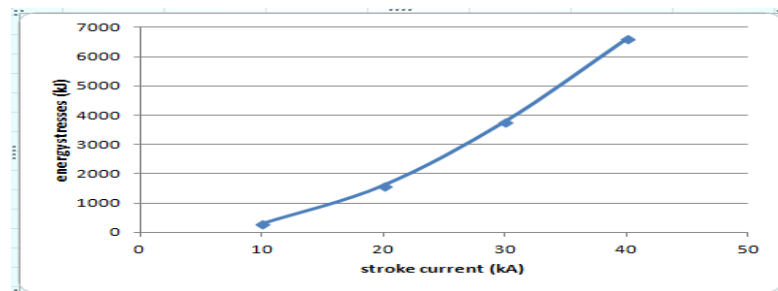


Figure 9: Effect of stroke currents magnitudes on MOSA energy stresses.

The energy stress of the MOSA is calculated when $1/50\mu\text{s}$ lightning stroke of a 30 kA peak current struck L2 at different distances from the GIS substation entrance. Fig.(10) shows the energy stress versus the distance of the striking point from GIS

substation entrance when the peak value of lightning current is 30 kA. It is observed that, as the distance increases, the energy stress on MOSA is decreased rapidly.

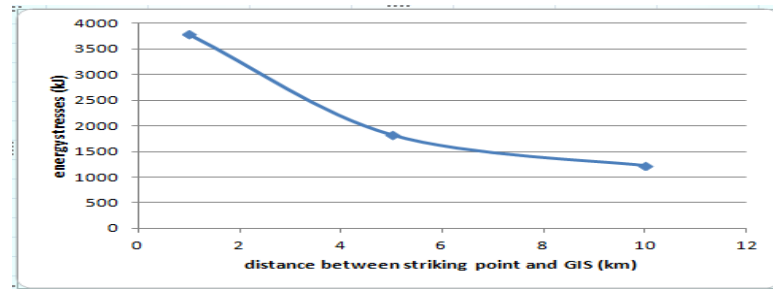


Figure 10: Effect of striking distance from GIS entrance on energy stress

The effect of the time of 20kA lightning impulse current wave front, with tail time 50 μ s, on the energy stress of MOSA is shown in Fig.(11). It is observed that, as the wave front time increases, the energy stress is decreased. The energy stress decreased to about 45% of its values as the wave front time increases from 1 μ s to 9 μ s. Fig.(12) shows the effect of the time of 20kA lightning impulse current wave tail, with front time 1 μ s, on the energy stress of MOSA. It is observed that, as the wave tail time increases, the energy stress is slightly increased. The energy stress increased by about 3.3% of its values as the wave tail time increases from 20 μ s to 80 μ s.

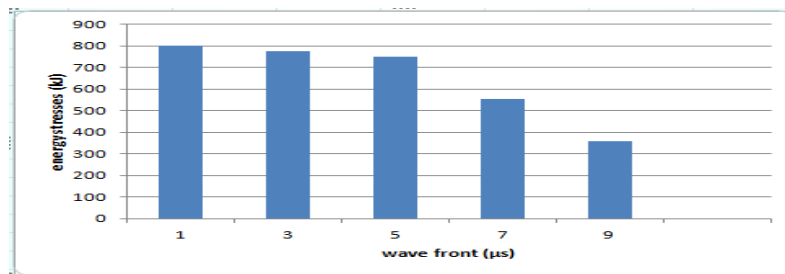


Figure 11: Effect of front time of the lightning stroke on MOSA energy stresses

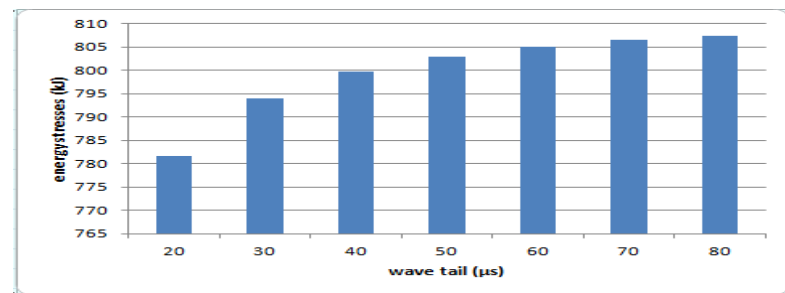


Figure 12: Effect of tail time of the lightning wave on MOSA energy stresses.

The effect of GIS substation terminations on the overvoltage transients and the energy stress of MOSA is presented and discussed at this section. Firstly, 100m length from each overhead line of the 220kV incoming feeders is replaced by underground cables. The 220 kV underground cable used is three single core XLPE Cu cable. JMARTI model has been used in the ATP package which also incorporates cable and sheath dimensions, resistivity and conductivity [11]. Fig.(13) shows the energy stresses on MOSA versus the striking distance from GIS substation terminal for 30 kA of 1/50 μ s lightning stroke, when 100 m cables are used at the two incoming feeders (i.e. GIS substation-Tebbin feeders). It is clear that, the using of underground cables decreases the energy stress on MOSA to about 66% of its value. Also, it is found that the energy stress decreases rapidly, as the striking distance increased. The energy stress is decreased to about 35% from its value as the striking distance increased from 1.0km to 10.0km. The underground cables are connected to all feeders connected to the GIS substation and their effects are shown in Fig.(14). The figure shows that, connecting the cables to all feeders reducing the energy stress to about 18% from its value. Also, it is found that the energy stress decreases rapidly, as the striking distance increased. The energy stress is decreased to about 19% from its value as the striking distance increased from 1.0km to 10.0km.

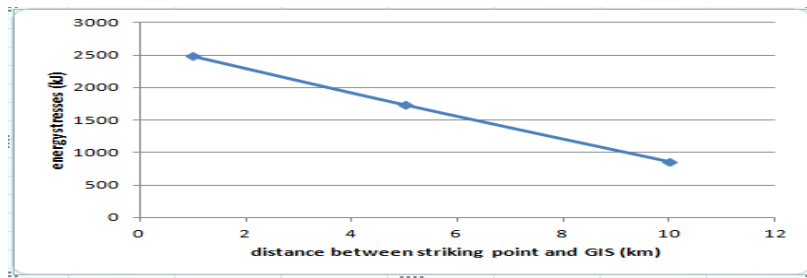


Figure 13: Effect of using 100 m cable at the incoming feeders from Tebbin

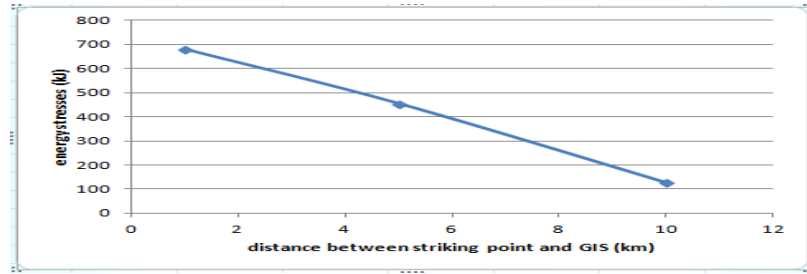


Figure 14: Effect of using 100 m cable at all connected feeders

A gas insulated lines (GIL) instead of underground cables are connected to the termination of the GIS substation and their effects are presented at this section. 220 kV GILs, each of 100 m length are connected to the incoming feeders terminals. The 220 kV GIL used is three single core GIL. Fig.(15) shows the energy stresses on MOSA versus the striking distance from GIS substation terminal for 30 kA of 1/50 μ s lightning stroke, when 100 m GILs are used at the two incoming feeders (i.e. GIS substation-Tebbin feeders). It is shown that, the using of GILs decreases the energy stress on MOSA to about 71.4% of its value. Also, it is found that the energy stress decreases rapidly, as the striking distance increased. The energy stress is decreased to about 32% from its value as the striking distance increased from 1.0km to 10.0km. The GILs are connected to all feeders connected to the GIS substation and their effects are shown in Fig.(16). The figure shows that, connecting the cables to all feeders reducing the energy stress to about 26.7% from its value. Also, it is found that the energy stress decreases rapidly, as the striking distance increased. The energy stress is decreased to about 18.8% from its value as the striking distance increased from 1.0km to 10.0km.

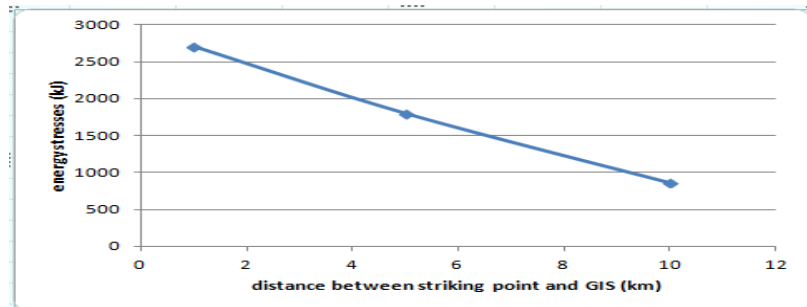


Figure 15: Effect of using 100 m GIL at the incoming feeders from Tebbin

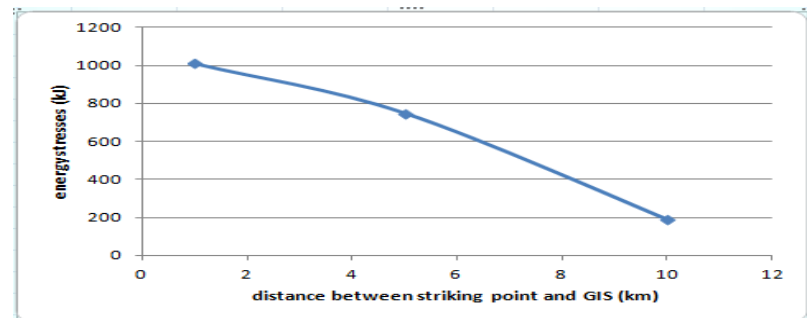


Figure 16: Effect of using 100 m GIL at all incoming feeders

VI. CONCLUSION

A 1/50 μ s Lightning stroke was hitting the incoming feeder with different magnitudes and at different distances from GIS entrance were simulated. The effect of the wave front and wave tail times of lightning stroke on energy stress of MOSA were discussed. The effect of different types of terminations for the GIS substation terminals on energy stress of MOSA was examined. The following conclusions were extracted.

1. As the striking point distance from GIS entrance increases, the energy stresses on MOSA is decreased.
2. As the front time of lightning stroke increases, the energy stresses on MOSA is decreased.
3. As the tail time of lightning stroke increases, the energy stresses on MOSA is increased.
4. The using of 100m cables in the two incoming feeders decreases the energy stress on MOSA to about 66% of its value, while using cables in all feeders reduces the energy stress to about 18% of its value.
5. The using of 100m GILs in the two incoming feeders decreases the energy stress on MOSA to about 71.4% of its value, while using GILs in all feeders reduces the energy stress to about 26.7% of its value.
- 6.

REFERENCES

- [1] IEC 60071-1:2006, "Insulation co-ordination – Part 1: Definitions, principles and rules", 2006.
- [2] CIGRE WG33.0, "Guide to procedure for estimating the lightning performance of transmission lines", CIGRE brochure 63, October 1991.
- [3] M. Gumede and G Frederick d'Almaine , "Surge Arrester Faults and Their Causes at EThekwini Electricity", International Journal of Electrical Energy, Vol. 2, No. 1, March 2014.
- [4] D.S. Pinches and M. A. Al-Tai, "Very Fast Transient Overvoltages Generated by Gas Insulated Substations", universities Power Engineering Conference, UPEC. 43rd International, 1-4 Sept. 2008.
- [5] A. Said, Ebrahim A. Badran and M. A. Abd-Allah, "Mitigation of Very Fast Transient Overvoltages at the More Sensitive Points in Gas-Insulated Substation", International Journal on Electrical Engineering and Informatics, Volume 4, Number 3, October 2012.
- [6] M. Kondalu1, Sreekanth Reddy Gillella and P.S. Subramanyam, "Analysis and Calculation of Very Fast Transient over Voltages in 220kv Gas Insulated Substation", Int J Engg Techsci, Vol 2(4), pp.314-319, 2011.
- [7] Mariusz Stosur, et. al., "GIS Disconnecter Switching Operation – VFTO Study", Modern Electric Power Systems , Wroclaw, Poland, 2010
- [8] IEEE Fast Front Transients Task Force, "Modeling guidelines for fast front transients", IEEE Trans. Power Delivery, Vol. 11, pp. 493–506. 1996.
- [9] Engjell Zeqo1, Rajmonda Bualoti and Olgert Metko, "Impact of replacement of conventional recloser with PulseCloser", ATI, April 2011
- [10] Shehab Abdulwadood ALI , "Design of Lightning Arresters for Electrical Power Systems Protection", POWER ENGINEERING AND ELECTRICAL ENGINEERING VOLUME: 11 , NUMBER: 6 , 2013
- [11] A. Elmitwally, S. Mahmoud, and M. H. Abdel-Rahman, "Fault Identification of Overhead Transmission Lines Terminated with Underground Cables", 14th International Middle East Power Systems Conference (MEPCON'10), Egypt, Paper ID 202, December 19-21, 2010.

AUTHORS

First Author – M. A. Abd-Allah, Electrical Engineering Department, Faculty of Engineering at Shoubra, Benha University. E-mail: mousa.abdullah@feng.bu.edu.eg

Second Author– M.S. El-Bages, Electrical Engineering Department, Faculty of Engineering at Shoubra, Benha University. E-mail: ph_mohamed@yahoo.com

Third Author – T. Elyan, qualifications, Electrical Engineering Department, Faculty of Engineering at Shoubra, Benha University. E-mail: tamerhamama@yahoo.com

Correspondence Author –, Amira.G.Nawar Electrical Engineering Department, Faculty of Engineering at Shoubra, Benha University. E-mail: eng_amira.2009@yahoo.com